Conformational Change of the Cation−Anion Pair of an Ionic Liquid Related to Its Low-Temperature Solid-State Phase Transitions

Sándor Kunsági-Máté,*,† Beáta Lemli,† Géza Nagy,†,‡ and László Kollár‡,§

Departments of General and Physical Chemistry and of Inorganic Chemistry, University of Pécs, and MTA-PTE Research Group for Chemical Sensors, Pécs, Hungary

Received: December 19, 2003; In Final Form: February 18, 2004

A first-principles ab initio density functional and semiempirical molecular dynamics study on the recently discovered low-temperature crystalline to crystalline phase transition of the 1-methyl-3-tetradecylimidazolium hexafluorophosphate ($[C_{14}mim]^+[PF_6]^-$) was performed. The results show that the experimentally obtained thermally activated change of the *a*, *b*, and *c* unit cell dimensions basically relates to two different facts. At an increased temperature the longest dimension *c* is lengthened by increased atomic motions inside the alkyl chain in accordance with the experiments. However, earlier experiments have shown that the dimension *a* was increased while, curiously, the *b* dimension was shortened with increasing temperature. Our results show that this unexpected change can be explained by the interconversion of two stable conformations of the $[C_{14}mim]^+[PF_6]^-$ pair. Related molecular dynamic simulation supports this observation.

1. Introduction

Ionic liquids (ILs) represent a fascinating class of molten salts that are liquid at and below 100 °C. These materials have attracted much attention especially in the past few years due to their wide applicability in the chemistry associated with a versatile environmentally neutral property.[1] While the preparation and properties of ILs were first published already a century ago,[2] sporadic results appeared on their application as reaction media until the 1980s, when an intensive search for alternative solvents started. Since that time, ILs have been known as a very interesting solvent class for many reasons. Their nonvolatile behavior avoids basic contamination problems, and furthermore, they are generally compatible with a wide range of reagents.[3,4] The flexibility of ILs as solvents has been clearly shown also in biphase catalytic reactions,[5,6] since their bicomponent phase diagram together with another green solvent, supercritical carbon dioxide, offers improved performance.[7] These materials are also widely used in homogeneous catalysis,[8] electrochemistry,[9] photochemistry,[10−12] and several separation techniques.[13] Although all of these interesting and unique properties could relate to the protection of natural resources, recent works,[14,15] where the hydrolysis of 1-butyl-3-methylimidazolium hexafluorophosphate was shown, highlighted that ILs are not always so "green". ILs must be treated much as one would any other research chemical with potentially hazardous properties or unknown toxicity or stability.[16]

To optimize the practical performance of ILs, detailed knowledge about the physical and chemical properties is required; especially structural parameters are needed to describe the interesting processes at the molecular level. Although quantum chemistry is one of the fruitful testing techniques for molecular-scale analysis, only a few computational or theoretical studies on ILs can be found in the literature. High-level quantum-chemical studies on the isolated cation and anion of ILs,[17,18] molecular dynamics,[19−22] and Monte Carlo simulations[23] on the liquid-phase structure appeared recently. One work deals with the phase transition, where the crystalline to liquid phase transition was examined by the MM+ force field and AM1 semiempirical quantum-chemical method.[24] The melting points derived from theoretical calculations were found to be comparable to the melting points of several ILs determined experimentally.

In a recent experimental work a wide range of analytical techniques were applied to characterize the phase behavior of 1-methyl-3-tetradecylimidazolium hexafluorophosphate ($[C_{14}mim]^+[PF_6]^-$).[25] The known typical phase transitions, such as crystalline to smectic, smectic to nematic, and nematic to isotropic, were identified in agreement with those reported by Gordon et al.[26] Furthermore, for the first time in the case of ILs, a low-temperature phase transition is found, which is assigned to a crystalline to crystalline transition. De Roche et al. showed[25] that in the higher temperature crystalline phase the $[C_{14}mim]^+$ cation has greatly increased freedom in its long alkyl chain and also on the anion compared to that of the lower temperature crystalline phase. In addition, the unit cell dimensions during transition from the lower to higher temperature crystalline phase are changed as follows: the longest axis is lengthened, while the shortest and the medium axes are interchanged, reflecting the change of the molecular conformation.

In this work we examine this crystalline to crystalline phase transition at the molecular level by quantum-chemical methods. Doing that, the conformational analysis on the stable conformations of $[C_{14}mim]^+[PF_6]^-$ (Figure 1) ionic liquid at different temperatures is performed. High-level ab initio density functional (DFT) calculations followed by semiempirical AM1 molecular dynamic analysis have been carried out to describe which molecular conformations are involved in the crystalline to crystalline phase transition and how the phase transition occurs.

† Department of General and Physical Chemistry, University of Pécs.
‡ MTA-PTE Research Group for Chemical Sensors.
§ Department of Inorganic Chemistry, University of Pécs.

10.1021/jp037933c CCC: $27.50
Published on Web 05/26/2004

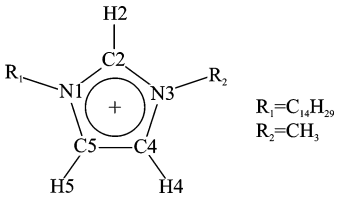

Figure 1. The 1-methyl-3-tetradecylimidazolium cation investigated in this work.

2. Calculation Methods

The equilibrium conformations of the $[C_{14}mim]^+[PF_6]^-$ ion pair and the separated ions were studied with the semiempirical AM1 (Austin model) method, followed by ab initio MP2/6-31G* and DFT/B3LYP/6-31G** (density functional theory) calculations. Polak−Ribiere and quadratic linear synchronous transit searches were used for geometry optimizations and transition-state (TS) calculations,[27,28] respectively. Verifying the existence of a true minimum, vibrational analysis was performed on all semiempirical and ab initio structures to ensure the absence of negative vibrational frequencies and also to check the transition-state virtual frequency. The crystal structure was analyzed by the Crystal Bilder implemented in the HyperChem package.[29] The temperature-dependent molecular dynamic simulations were performed at the semiempirical AM1 level. A 0.1 fs simulation time step was set because of the fast C−H vibrations. Ten thousand points were calculated in each run. Finding an appropriate initial condition for molecular dynamics, a "heating" algorithm implemented in HyperChem[29] was used. This procedure heats the molecular system smoothly from lower temperatures to the temperature T at which it is desirable to perform the final molecular dynamics simulation. The starting geometry for this heating phase is a static initial structure. We used the optimized AM1 geometry as an initial structure, and the temperature step and the time step in the heating phase were set to 2 K and 0.1 fs, respectively. For molecular dynamics performed on the larger system a periodic boundary with an AMBER force field[30] was used. In this case a periodic box imposes periodic boundary conditions on the calculations. Periodic boundary conditions provide identical molecular systems which are virtual images, identical to the one in the periodic box, surrounding the periodic box. For the purposes of the calculations, molecules can move in a constant-density environment. All types of calculations were carried out with the HyperChem Professional 7 program package.[29]

3. Results and Discussion

3.1. Conformation of the Separated Cation and Anion of the $[C_{14}mim]^+[PF_6]^-$ Ion Pair. The equilibrium conformation of the $[C_{14}mim]^+$ cation was determined by the AM1 method, and then, starting from this semiempirical structure, the conformation was calculated with the DFT/BLYP/6-31G* method. Table 1 summarizes the selected internal coordinates relevant to the imidazolium ring conformation.

Since the geometry of the imidazolium ring only slightly depends on the length of the alkyl chain, it can be compared with the results obtained for similar, but differently alkylated, imidazolium cations.[22,25,26,31,32] The data show good agreement with the theoretical results of de Andrade et al.,[22] which were determined at the UHF/6-31G(d) level for the 1-*n*-butyl-3-methylimidazolium cation. It can be clearly seen that the structures are also in satisfactory agreement with the X-ray data, especially considering that the X-ray data have been obtained from crystal structures whereas the calculations were done on an isolated imidazolium cation.

3.2. Dynamic Property of the $[C_{14}mim]^+$ Cation. Effect of the Temperature on the Alkyl Chain Length. The crystalline to crystalline phase transition, found recently for 1-methyl-3-tetradecylimidazolium hexafluorophosphate, was obtained at 278 K.[25] Therefore, to obtain changes on the dynamics of motion on the alkyl chain of the $[C_{14}mim]^+$ cation, the simulation temperatures were chosen either above (300 K) or below (175 K) this transition temperature. These temperatures were chosen according to the experimental setup[25] for later comparison. During these calculations, after the heating phase, a 100 fs equilibration period was used, and then 10000 data points during a 1 ps time interval and with 0.1 fs resolution were recorded. The qualitative analysis of the distribution of vibrational energy localized on the bonds of the molecule was described as follows.[33,34] Using the data collected above, the average amplitude of vibration was derived as the standard deviation of the regarded bond stretching data points from the average bond lengths. Using these amplitudes and the appropriate bond stretching frequencies, the vibrational energy localized on a given bond was estimated by definition of an oscillator. Then, the total vibration energy was normalized to unity.

Figure 2 shows the vibrational energy distribution on the carbon atoms of the alkyl chain and of the methyl group attached to the N3 nitrogen atom. The two curves show the distribution at two temperatures below and above the transition temperature. The vibrational energy localized on the imidazolium ring was

TABLE 1: Geometrical Parameters Selected for the Imidazolium Ring of the $[C_{14}mim]^+$ Cation

parameter[a]	DFT/B3LYP	UHF/6-31G(d)[b]	X-ray[c]	X-ray[d]	X-ray,[e] 175 K (300 K)	X-ray,[f] 123 K
			Bond Lengths			
N1−C2	1.334	1.314	1.31	1.332	1.31 (1.31)	1.32
C2−N3	1.336	1.316	1.28	1.334	1.28 (1.32)	1.32
N3−C4	1.374	1.378	1.39	1.369	1.37 (1.37)	1.37
C4−C5	1.357	1.342	1.30	1.355	1.29 (1.33)	1.33
C5−N1	1.374	1.378	1.42	1.373	1.36 (1.36)	1.36
			Bond Angles			
C2−N1−C5	107.6	107.9	111	109.0	107.36 (108.30)	107.87
N3−C2−N1	109.8	109.9	108	107.9	111.15 (107.46)	108.74
C4−N3−C2	108.0	108.0	107	109.2	105.50 (107.32)	108.54
C5−C4−N3	107.1	107.0	108	106.9	109.83 (107.88)	106.99
N1−C5−C4	107.1	107.2	101	107	106.12 (109.01)	107.83

[a] Bond lengths and bond angles are in angstroms and degrees, respectively [b] Theoretical parameters for the imidazolium ring of 1-*n*-butyl-3-methylimidazolium.[22] [c] Experimental parameters for the imidazolium ring of 1-ethyl-3-methylimidazolium.[31] [d] Experimental parameters for the imidazolium ring of 1-*n*-butyl-3-methylimidazolium.[32] [e] Experimental parameters for the imidazolium ring of 1-*n*-tetradecyl-3-methylimidazolium.[25] [f] Experimental parameters for the imidazolium ring of 1-*n*-dodecyl-3-methylimidazolium.[26]

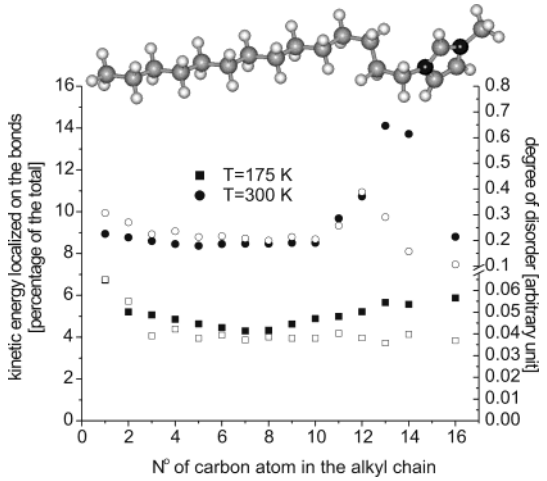

Figure 2. Kinetic energy localized in the closest environment of carbon atoms in the alkyl chain (solid symbols). Carbon atoms are numbered from the terminated end of the chain. Numbers 14 and 16 refer the carbon atoms of the methylene group adjacent to N1 and that of the methyl group adjacent to N3, respectively. The C−H stretch energy and half of the C−C stretch energy related to a given atom are summed up. Data for 300 K were normalized to the total kinetic energy at 175 K. Bond bending and dihedral vibrations are omitted from the calculation. The ring total vibrations were calculated, but omitted from the figure (see the text). Open symbols reflect the experimental data of De Roche et al.[25]

omitted. The curves show a temperature-induced redistribution of the kinetic energy on the alkyl chain which results in increased motions of the carbon and hydrogen atoms the closest to the imidazolium ring. This observation is in agreement with the results obtained from the small- and wide-angle X-ray (S-WAXS) diffraction method.[25] The length of the molecule was described with the average distance between the two terminated carbon atoms (i.e., the methyl carbon of the C14 chain and the methyl carbon attached to N3) during the 1 ps simulation time when the geometry was sampled. This distance was found to be 19.72 Å at 175 K and increased to 20.72 Å at 300 K. This means that the increased temperature induces a 5.07% increase in the length of the molecule.

In the crystalline phase, the structure of this IL shows a monodispersed layer with interdigitated alkyl chains. The distance of these layers (namely, the *d*-spacing) was found to be equivalent with the *c* dimension of the unit cell; i.e., the alkyl chains are situated in an orthogonal position to the layers. For the *c* parameter 24.2 Å was found by the X-ray method at 175 K, which increased to 25.4 Å at 300 K. This means a 4.96% increase in the *d*-spacing, in agreement with our theoretical result. Note that the *c* measure is the longest axis of the unit cell (see later) and *c* is the sum of the length of the molecule plus the thickness of the "empty" field between two interdigitated layers.

3.3. Search Models for the Possible Stable Conformations of the $[C_{14}mim]^+[PF_6]^-$ Ion Pair. An intuitive search, however, also under the suggestion of Meng et al.[18] for the possible stable conformers of the $[C_{14}mim]^+[PF_6]^-$ ion pair was performed as follows: PF_6^- was positioned in various locations selected at four actual directions around the imidazolium moiety, on the two opposite sides and one up and one down. Using these starting conformations, geometry optimizations were done with the AM1 method and afterward by DFT calculations. We found stable conformations only when the phosphorus atom of the hexafluorophosphate anion lies nearly in the plane of the imidazolium ring and close to its H2 hydrogen atom. This is in agreement with the experimental results reported recently;[25]

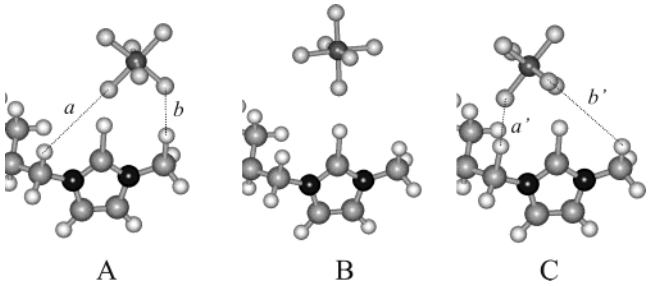

Figure 3. Stable conformations of the $[C_{14}mim]^+[PF_6]^-$ pair (A and C) and the transition-state conformation (B) related to the transition between these two stable conformations. Dotted lines show the H···F distances used for the comparison of the X-ray and theoretical data. The alkyl chain (left) was omitted for clarity.

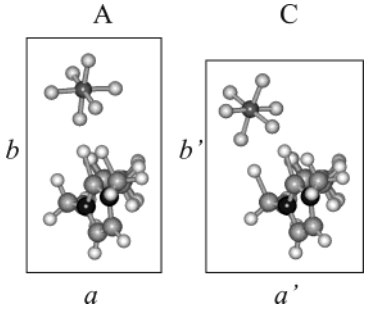

Figure 4. Top view of the two stable (A and C) conformations of the $[C_{14}mim]^+[PF_6]^-$ ion pair. Letters *a* and *b* mark the shorter two unit cell dimensions.

however, it disagrees with the results reported earlier for the 1-butyl-3-methylimadazolium hexafluorophosphate system,[18] since in that work stable conformations were found in all the cases listed above. In the plane of the imidazolium ring we found two stable conformations (Figure 3A,C). In both cases the H2 hydrogen connected to the C2 carbon of the imidazolium ring was involved in forming the stable conformation. The C2−H2 bond, however, appeared highly extended (bond length ∼1.78 Å). It is only 1.17 Å in the free imidazolium cation. This is consistent with the acidity of the H2 hydrogen and also shows that this hydrogen atom is involved in the hydrogen bonding of the cation−anion pair of the ionic liquid. Another hydrogen bond between the imidazolium moiety and the hexafluorophosphate anion supports the ion pair formation. In this, either one of the hydrogen atoms of the methyl group (Figure 3A) or one hydrogen atom of the alkyl side chain is involved (Figure 3C). In the A and C conformations the CH bonds on the methyl or alkyl chain show increased bond lengths, 1.55 Å and 1.59 Å, respectively. The interaction energy, i.e., the stability, was calculated as the difference of the total energy of the $[C_{14}mim]^+[PF_6]^-$ pair and that of the separated ions. The stabilities of the $[C_{14}mim]^+[PF_6]^-$ system in the two stable conformations (A and C) are different. While the $[C_{14}mim]^+$-$[PF_6]^-$ pair has a stabilization energy of −353 kJ/mol in the C conformation, the A state shows a greater, −367 kJ/mol, stabilization energy. The latter value is in very good agreement with the same value of 1-butyl-3-methylimidazolium hexafluorophosphate determined in the same way (−370 kJ/mol[18]). These two stable conformations are separated by an energy barrier of 43 kJ/mol. Starting from structure A, which could be related to a lower temperature, the system can overtake the barrier at structure B by, e.g., thermal activation, and finally reaches the stable A structure, which, because of its higher energy, could be related to a higher temperature equilibrium. We have to note, however, that the conformations calculated above show deviations from the experimental X-ray data. Although the displace-

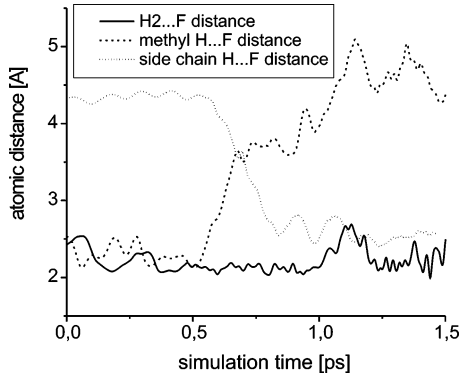

Figure 5. Mechanistic details for the transition between the two stable conformations A and C.

ment of the hexafluorophosphate anion observed experimentally between the low (175 K) and high (300 K) temperature crystalline phases agrees well with our calculations, the experiments show smaller displacement.

For quantitative comparison of the experimental and theoretical results in the A and C states, we describe the anion position with the closest H···F distances between the fluorine atoms of the anion and either one of the hydrogen atoms of the methyl group (Figure 3, lines *b* and *b*′) or one hydrogen atom of the alkyl side chain (Figure 3, lines *a* and *a*′). The (*a*, *b*) and (*a*′, *b*′) values were measured[25] as (2.72 Å, 2.62 Å) and (2.86 Å, 2.98 Å) and were calculated as (3.51 Å, 2.76 Å) and (2.87 Å, 3.53 Å), respectively. The discrepancies between the theoretical and experimental results could arise either from the absence of the periodic boundary or from the "static" behavior of the calculations. The latter highlights that an averaging of the conformations by molecular dynamics would be necessary for further quantitative comparison in this case. It, however, would take enormous CPU time at the ab initio level.

3.4. Consequences of the Conformational Changes on the Unit Cell Dimensions of the $[C_{14}mim]^+[PF_6]^-$ Ionic Liquid. In the crystalline phase, the structure of the ILs is layered with interdigitated alkyl chains of the imidazolium cation. The alkyl chains are closely perpendicular to the interface of the layers. The layer by layer distance was identified as the *c* dimension of the unit cell. The other two unit cell dimensions, *a* and *b*, lie parallel to the layers since an orthorhombic crystal structure can be assumed from the experimental investigation.[25] The variation of the dimension *c* under the effect of increased temperature was discussed above.

Figure 4 shows the variation of the unit cell dimensions *a* and *b* in accordance with the two stable conformations of the $[C_{14}mim]^+[PF_6]^-$ pair. It can be seen clearly that the change

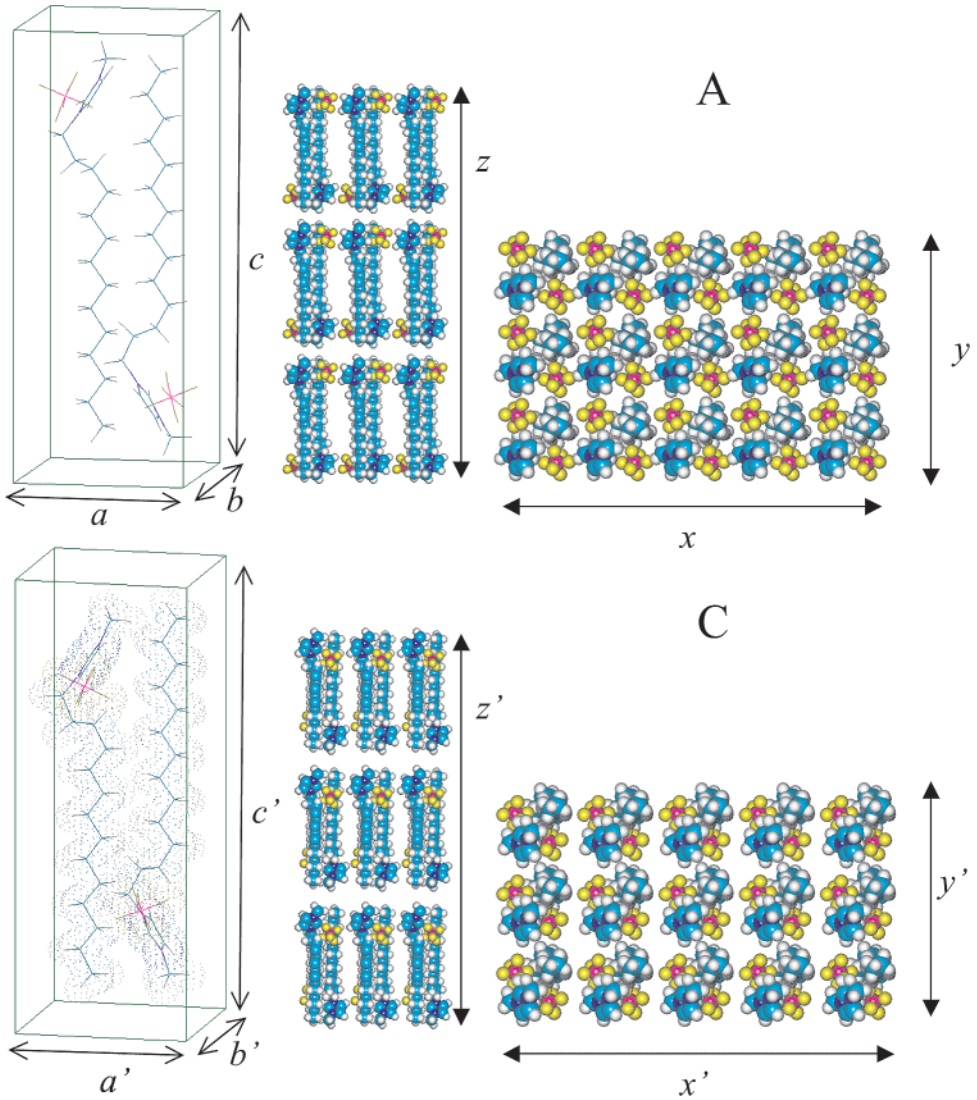

Figure 6. A larger view of the $[C_{14}mim]^+[PF_6]^-$ crystal. *a*, *b*, and *c* are the dimensions of the unit cell associated with the A conformation, while *a*′, *b*′, and *c*′ represent the unit cell dimensions in the C conformation. *x*, *y*, and *z* and *x*′, *y*′, and *z*′ refer to the larger appropriate dimensions.

from the lower energy conformation A to conformation C, which has a higher energy, results in an increase and in a decrease of the *a* and *b* unit cell dimensions, respectively. Figure 4 also shows that this effect is essentially based on the tilted orientation of the imidazolium ring relating to its connected alkyl chain.

3.5. Mechanistic Details of the Conformational Change Related to the Dynamics of a Crystalline to Crystalline Phase Transition. To obtain the possible effect of an increased temperature on the interchange between the A and C conformations (see Figure 3), a molecular dynamic calculation was done using the AMBER force field.[30,22] During these calculations, after the system was heated to 250 K by the procedure described in the Calculation Methods, a 100 fs equilibration period was used, and then a heating with 0.1 K/ps was performed. The atomic distances were recorded with 0.1 fs resolution.

Figure 5 shows the temporal variations of the distances between the appropriate hydrogen atoms of the imidazolium cation and fluorine atoms of the hexafluorophosphate anion that are the closest to the mentioned hydrogens. Although several runs were done, Figure 5 shows an example when the adequate distances are plotted against the simulation time just when the transition between the A and B states occurs. The appropriate temperature for the phase transition was measured as 263 K; however, it was different during different runs. The simulated transition temperature was varied from about 255 to 285 K. Surprisingly, these theoretical values are close to the experimental value determined as the crystalline to crystalline phase transition temperature (278 K) especially if we consider that the data were obtained from the force field calculation. However, we are not able to compare the theoretical and experimental values, since only one cation−anion pair was considered during this molecular dynamic simulation.

3.6. Crystal Structure Supposed from the Structural Change Obtained in the Individual $[C_{14}mim]^+[PF_6]^-$ Ion Pair. Figure 6 shows a schematic larger view of the $[C_{14}mim]^+[PF_6]^-$ crystal. The part of the crystal shown in the figure was produced by the HyperChem Crystal Builder. To equilibrate the molecules in the unit cell, AMBER force field with periodic boundary conditions was applied.[22,30] The two cases, one with the hexafluorophosphate anions located closer to the methyl substituent of the imidazolium ring (A) and the other one with the anion located closer to the alkyl chain (C), were drawn. The changes in the unit cell described above can be seen clearly in Figure 6. *a*, *b*, and *c* are the dimensions of the unit cell associated with the A conformation, while a', b', and c' represent the unit cell dimensions in the C conformation. When an A to C transition occurs, the dimensions of the unit cell change as described above, showing $a' > a$, $b' < b$, and $c' > c$ relations. Naturally, the larger dimensions *x*, *y*, and *z* and x', y', and z' change accordingly. The figure also shows that the hexafluorophosphate anion lies more deeply in the layers formed by the interdigitated $[C_{14}mim]^+[PF_6]^-$ pair. We note here that in our calculations the alkyl chain in the unit cell is tilted with an angle of about 8° to the *c* axis of the unit cell, while it is closely parallel to the *c*−*b* plane.

4. Conclusions

The recently discovered low-temperature crystalline to crystalline phase transition of $[C_{14}mim]^+[PF_6]^-$ was examined by ab initio density functional and semiempirical molecular dynamics calculations. Our results showing a change in the basic structure of this IL are in very good agreement with the conclusion of a recently published paper,[25] but in contrast with its interpretation of the crystalline to crystalline phase transition of the $[C_{14}mim]^+[PF_6]^-$ ionic liquid. The results show that during the thermally activated phase transition the longest dimension of the unit cell (*c*) was extended due to the increased atomic motions inside the alkyl chain, in agreement with the experiments.[25] However, earlier experiments have shown that the unit cell dimension *a* increases while, curiously, the *b* dimension decreases with increasing temperature. It was suggested that the crystalline to crystalline phase transition does not involve a major structural change, but it is largely marked by an increase in the degree of motion in the anion and the alkyl chain. Our results show that this unexpected change is associated with an interconversion between two stable conformations of the $[C_{14}mim]^+[PF_6]^-$ ion pair. Molecular dynamic simulation presented in this work for the transition at higher temperature supports that in this particular case the ILs show polymorphic crystalline character.

Acknowledgment. The financial support of the Hungarian Scientific Research Fund (OTKA Grant TS044800) is highly appreciated.

References and Notes

(1) Holbrey, J. D.; Seddon, K. R. *Clean Prod. Processes* **1999**, *1*, 223.
(2) Walden, P. *Bull. Acad. Imper. Sci. (St. Petersburg)* **1914**, 1800.
(3) Welton, T. *Chem. Rev.* **1999**, *99*, 2071.
(4) Wasserscheid, P.; Kleim, W. *Angew. Chem., Int. Ed.* **2000**, *39*, 3772.
(5) Gordon, C. M. *Appl. Catal., A* **2001**, *222*, 101.
(6) Sheldon, R. *Chem. Commun.* **2001**, 2399.
(7) Holbrey, J. D.; Seddon, K. R. *J. Chem. Soc., Dalton Trans.* **1999**, 2133.
(8) Skoda-Földes, R.; Takács, E.; Horváth, J.; Tuba, Z.; Kollar, L. *Green Chem.* **2003**, *5* (5), 643.
(9) Hussey, C. L. In *Chemistry of Nonaqueous Solutions*, Mamantov, G., Popov, A. I., Eds.; VCH: Weinheim, Germany, 1994; p 227.
(10) Gordon, C. M.; McLean, A. J. *Chem. Commun.* **2000**, 1395.
(11) Karmakar, R.; Samanta, A. *J. Phys. Chem. A* **2003**, *107*, 7340.
(12) Chakrabarty, D.; Hazra, P.; Chakraborty, A.; Seth, D.; Sarkar, N. *Chem. Phys. Lett.* **2003**, *381*, 697.
(13) Visser, A. E.; Swatlowski, R. P.; Rogers, R. D. *Green Chem.* **2000**, *2*, 1.
(14) Rangits, G.; Petöcz, G.; Berente, Z.; Kollár, L. *Inorg. Chim. Acta* **2003**, *353*, 301.
(15) Swatloski, R. P.; Holbrey, J. D.; Rogers, R. D. *Green Chem.* **2003**, *5* (4), 361.
(16) Kosmulski, M.; Gustafsson, J.; Rosenholm, J. B. *Thermochim. Acta*, in press.
(17) Takahashi, S.; Suzuya, K.; Kohara, S.; Koura, N.; Curtiss, L. A.; Saboungi, M.-L. *Z. Phys. Chem.* **1999**, *209*, 209.
(18) Meng, Z.; Dölle, A.; Carper, W. R. *J. Mol. Struct.: THEOCHEM* **2002**, *585*, 119.
(19) de Andrade, J.; Böes, E. S.; Stassen, H. *J. Phys. Chem. B* **2002**, *106*, 3546.
(20) Hanke, C. G.; Atamas, N. A.; Lynden-Bell, R. M. *Green Chem.* **2002**, *4*, 107.
(21) Hanke, C. G.; Price, S. L.; Lynden-Bell, R. M. *Mol. Phys.* **2001**, *99*, 801.
(22) de Andrade, J.; Böes, E. S.; Stassen, H. *J. Phys. Chem. B* **2002**, *106*, 13344.
(23) Shah, J. K.; Brennecke, J. F.; Maginn, E. J. *Green Chem.* **2002**, *4*, 112.
(24) Katritzky, A. R.; Lomaka, A.; Petrukhin, R.; Jain, R.; Karelson, M.; Visser, A. E.; Rogers, R. D. *J. Chem. Inf. Comput. Sci.* **2002**, *42*, 71.
(25) De Roche, J.; Gordon, C. M.; Imrie, C. T.; Ingram, M. D.; Kennedy, A. R.; Lo Celso, F.; Triolo, A. *Chem. Mater.* **2003**, *15*, 3089.
(26) Gordon, C. M.; Holbrey, J. D.; Kennedy, A. R.; Seddon, K. R. *J. Mater. Chem.* **1998**, *12*, 2627.
(27) Dewar, J. S.; Dieter, K. M. *J. Am. Chem. Soc.* **1986**, *108*, 8075.
(28) Peng, C.; Schlegel, H. B. *Isr. J. Chem.* **1993**, *33*, 449.
(29) HyperChem Professional 7, Hypercube, 2002.
(30) Cornell, W. D.; Cieplak, P.; Bayly, C. I.; Gould, I. R.; Merz, K. M., Jr.; Ferguson, D. M.; Spellmeyer, D. C.; Fox, T.; Caldwell, J. W.; Kollman, P. A. *J. Am. Chem. Soc.* **1995**, *117*, 5179.
(31) Elaiwi, A.; Hitchcock, P. B.; Seddon, K. R.; Srinivasan, N.; Tan, Y.-M.; Welton, T.; Zora, J. A. *J. Chem. Soc., Dalton Trans.* **1995**, 3467.
(32) Dupont, J.; Suarez, P. A. Z.; de Souza, R. F.; Burrow, R. A.; Kintzinger, J.-P. *Chem.—Eur. J.* **2000**, *6*, 2377.
(33) Kunsági-Máté, S.; Végh, E.; Nagy, G.; Kollár, L. *J. Phys. Chem. A* **2002**, *106*, 6319.
(34) Kunsági-Máté, S.; Végh, E.; Nagy, G.; Kollár, L. *Chem. Phys. Lett.* **2004**, *388*, 84.